Biogeochemistry (2012) 108:27–38
DOI 10.1007/s10533-010-9570-y

The influence of tidal forcing on groundwater flow and nutrient exchange in a salt marsh-dominated estuary

Alicia M. Wilson · James T. Morris

Received: 27 May 2010 / Accepted: 29 December 2010 / Published online: 15 January 2011

Abstract Data from salt marshes in the U.S. Southeast show that long-term variations in mean water level (MWL) correlate strongly with salt marsh productivity and porewater salinity. Here we used numerical models of tidally-driven groundwater flow to assess the effect of variations in tidal amplitude and MWL on porewater exchange between salt marshes and tidal creeks. We modeled homogeneous and layered stratigraphy and compared flat and sloped topography for the marsh surface. Results are consistent with field observations and showed that increases in tidal amplitude increased groundwater flushing, particularly when increasing the tidal amplitude caused the marsh platform to be inundated at high tide. Increases in MWL caused groundwater flushing to increase if that rise caused greater areas of the marsh to be inundated at high tide. Once the marsh was fully inundated at high tide, further increases in MWL caused groundwater flushing to decrease. Results suggest that small increases in MWL associated with sea level rise could increase nutrient export significantly in marshes with elevations that are equilibrated near mean high water, but rising sea level could decrease the export of nutrients to, and thus fertility in, estuaries adjacent to marshes that are equilibrated lower in the tidal frame. Likewise, macrotidal estuaries are predicted to be subject to much larger groundwater and nutrient exchange than similar microtidal estuaries. We speculate that the early stages of rising relative sea level may significantly impact water quality in estuaries that are not river-dominated by raising the discharge of nutrients from coastal wetlands.

Keywords Wetlands · Nutrient cycling · Spartina · Tides · Numerical models · Groundwater

A. M. Wilson (✉)
Department of Earth and Ocean Sciences, University of South Carolina, Columbia, SC 29208, USA
e-mail: awilson@geol.sc.edu

J. T. Morris
Department of Biological Sciences, University of South Carolina, Columbia, SC 29208, USA
e-mail: morris@biol.sc.edu

Introduction

Groundwater flow is an important component of salt marsh ecosystems. Spatial and temporal variations in the height of the water table below the sediment surface alter the saturation and redox state of subsurface sediments, which influence salt marsh productivity (e.g. Howes et al. 1981). Groundwater flow also controls sediment salinity, which is a particularly important determinant of salt marsh primary production and zonation (Morris 1995; Gardner and Reeves 2002). Groundwater flow in salt marsh sediments also affects nutrient cycling in salt

marshes and adjacent surface waters, because groundwater draining from salt marsh sediments at low tide is greatly enriched in nutrients compared to surface water (Whiting and Childers 1989).

Groundwater flow rates and patterns within individual marshes are controlled by tidal fluctuations, evapotranspiration, precipitation, discharge from adjacent freshwater uplands, and the geometry and hydraulic properties of the marsh sediments. Of these factors, tidal fluctuations are the most widely important driver for groundwater exchange. Given this importance, it is reasonable to expect that variations in the tidal signal could affect salt marsh primary production and biogeochemical cycles.

Tidal signals vary significantly over multiple timescales. Variability in wind and atmospheric pressure alter mean water level (MWL) over time scales of days (storm surge). MWL also varies with sea temperature, which fluctuates in response to seasonal and decadal climate and long-term global warming. Interactions among these factors can cause yearly changes in MWL to greatly exceed the long-term rate of sea-level rise (Stumpf and Haines 1998; Morris 2000). Changes in tidal amplitude add further to the variation in tidal signal, primarily over time scales of spring-neap (2-week) lunar cycles and 18.6 year lunar nodal cycles.

Previous field studies have revealed striking correlations between the depth of flooding by tides and salt marsh productivity, porewater salinity, and porewater nutrient concentrations (Morris 2000). Salt marsh productivity was positively correlated with July–August peaks in mean sea level in salt marshes at North Inlet, SC (Morris and Haskin 1990; Morris 2000). Increases in mean water level (MWL) also correlated with decreases in salinity, which is likely a proximal control on production (Morris 2000). Thus, at these sites, increasing MWL appears to have increased groundwater flushing, removing additional salts.

Harvey et al. (1987) used one-dimensional numerical models to explore the effects of variation in tidal amplitude and mean water level on groundwater flow. In simulations based on a Virginia salt marsh, increases in the elevation of mean water level relative to the top of the marsh platform caused significant decreases in the total volume of groundwater exchange over a tidal cycle, which appears to contradict the field results of Morris (2000). Increases in tidal amplitude increased flushing, and a 5 cm change in tidal amplitude had less of an effect than a 5 cm change in mean water level. Increases in the hydraulic conductivity of the sediments predictably increased groundwater exchange, but, as permeability rose, discharge became increasingly limited by the period of the tide rather than the permeability of the sediments (Harvey et al. 1987). As discussed in more detail below, however, the models relied on significant simplifications. More recently, 2-D numerical models developed by Wilson and Gardner (2006) showed that, for the same tidal amplitude, groundwater exchange in a simulated marsh was higher when the marsh was inundated by the tide than when it was not. That study, however, was not designed to explore the impact of tidal parameters on groundwater exchange, nor did it go beyond assuming simple homogeneous marsh sediments. Thus the impact of variations in MWL and tidal amplitude on groundwater exchange remains incompletely understood.

Here we use modern 2-D numerical models based on salt marshes of the U.S. southeastern coastline to systematically explore groundwater exchange rates for a range of tidal conditions and representative sediment types. We use the model to generalize about the effect of rising sea level on nutrient exchange between the marsh and adjacent tidal creeks. Long-term measurements of nutrients in marsh pore water and tidal creeks made at North Inlet estuary, SC, provide the context.

Numerical models of tidal exchange in salt marshes

Quantitative models of groundwater flow in marshes have advanced significantly over the last four decades. Although 2-D finite element models of tidal fluctuations were presented for sandy beach settings early in the 1970s (Fang et al. 1972), early models of salt marshes considered 1-D evapotranspiration (Hemond and Fifield 1982) and 1-D (horizontal) analytic solutions for the propagation of tidal fluctuations (Nuttle 1988). One limitation of the horizontal analytic solutions is that they could not simulate tidal flooding (Nuttle 1988). Tidal flooding causes 2-D flow and violates the common assumption that the total stress (the weight of water and sediments overlying the aquifer) remains constant (Reeves et al.

2000; Gardner and Wilson 2006). Harvey et al. (1987) worked around this problem by developing a numerical solution to a 1-D form of the transient groundwater flow equation. Tidal flooding was approximated by imposing no-flow conditions throughout the flooded area, and simulation results were consistent with field observations.

Subsequent studies have presented several different approaches for modeling 2-D flow in marshes. Most rely on a form of the Richards equation, which can be used to simulate saturated and unsaturated groundwater flow. The Richards approach may overestimate groundwater flow across the marsh surface when the marsh surface drains enough to allow significant air entry (Li et al. 2005), but the single phase Richards Equation is a good approximation for many marshes, which remain poorly drained even at low tide (Hemond and Fifield 1982). Two forms of the Richards equation have been applied in recent marsh studies. One form avoids the issue of variations in total stress by neglecting sediment compressibility

$$\nabla \cdot [K(\psi)\nabla h] = \frac{\partial \theta}{\partial t} \tag{1}$$

where K is hydraulic conductivity, ψ is capillary head (negative pressure head), h is hydraulic head, θ is water content (a function of ψ only), and t is time. In this approach fluid flow occurs due to hydraulic gradients and drainage of pore spaces. The other form of the equation incorporates sediment compressibility, fluid compressibility, and changes in total stress (Reeves et al. 2000)

$$\nabla \cdot [K(\psi)\nabla h] = S_w S_S \frac{\partial h}{\partial t} + \phi \frac{\partial S_w}{\partial t} - \alpha_s S_w \frac{\partial \sigma_T}{\partial t} \tag{2}$$

where S_w is water saturation, ϕ is porosity, σ_T is the total stress, and S_s is the specific storage,

$$S_S = \rho g(\alpha_s + \phi\beta) \tag{3}$$

where ρ is the density of water, g is gravity, α_s is sediment compressibility, and β is fluid compressibility.

Marsh sediments are typically highly compressible (Hemond and Fifield 1982), which suggests that it is important to include sediment compressibility. Gardner and Wilson (2006) compared the approaches, and their results suggest that compressible flow can indeed contribute significantly to the total volume of fluid exchange. They also found that governing equations that allow compressible flow but do not account for changes in total stress may overestimate total groundwater exchange by an order of magnitude or more. Note that two-phase models that incorporate compressibility are subject to the same error.

Three modeling studies have considered the volume of groundwater discharge from marshes since Harvey et al. (1987). Gardner (2005, 2007) used the Richards equation for incompressible flow to explore seepage patterns across the creek bank and bottom for a variety of marsh geometries and sediment properties, including systems in which marsh mud overlies sand, typical of many marshes in the southeastern U.S. These studies confirmed the basic findings of Harvey et al. (1987) and suggested that the success of the 1-D approach of Harvey et al. (1987) was likely due to the specific geometry of the marsh in question. Based on prior observations that the productivity of *Spartina alterniflora* is greatest on well-flushed creek banks (Valiela et al. 1978; Medelssohn et al. 1981; King et al. 1982; Medelssohn and Morris 2000), Gardner (2005) also speculated that marshes with higher permeability sediments and larger tidal amplitudes might have higher productivity. Wilson and Gardner (2006) incorporated sediment compressibility and variations in total stress due to tidal fluctuations into 2-D simulations using the Richards equation to illustrate flow paths and the extent of groundwater exchange within marsh sediments in a generic, homogeneous marsh platform. Results indicated an increase in groundwater exchange in a marsh that was inundated at high tide compared to a marsh that was not inundated at high tide, suggesting additional complications to the original results of Harvey et al. (1987). Here we revisit these findings, applying the modern modeling techniques of Wilson and Gardner (2006) to systematically explore links between groundwater discharge, tidal amplitude, and MWL.

Numerical models

Simulations of tidal fluctuations in a marsh platform were conducted using a version of SUTRA (Voss and Provost 2002) that was modified to solve Eq. 2 in two dimensions. The hydraulic conductivity was calculated (Gardner 1958)

$$K(\psi) = K_S e^{\alpha\psi} \quad (4)$$

where K_S is the saturated hydraulic conductivity and α is the inverse of the capillary rise. In these simulations the capillary rise was 1 m. Saturation was calculated

$$S_w = \left(1 - S_{w,r}\right)e^{\alpha\psi} + S_{w,r} \quad (5)$$

where $S_{w,r}$, the residual saturation, was assumed to be 0.60.

The simulation domain was based on two common marsh geometries observed in the U.S. southeast (Fig. 1). In the first configuration the marsh platform was horizontal, which is representative of the many marsh islands that have very little (<10 cm) surface topography. In the second configuration, the marsh platform sloped downward toward the creek, with a slope of 50 cm over 60 m. This configuration captures an important characteristic of fringing marshes, which is that high tides inundate a greater area of the marsh than lower tides do. The presence of a levee does not interfere with this effect, because levees are commonly broken by small tidal creeks that allow water onto the marsh platform behind the levee before the levee itself is inundated.

Boundary conditions on the upper surface of the simulation domain were specified based on tidal height. If the point in question was inundated, the pressure was specified based on the depth of the water column. If the point was exposed but the sediment was still saturated, the pressure was specified to be zero, allowing the formation of a seepage face. If the point was exposed and the pressure in the sediments was less than zero, a specified flux boundary was imposed to account for evapotranspiration and precipitation. Here we focus on the volume of water exchanged via tidal fluctuations, so net evapotranspiration and precipitation was set to zero. Infiltration associated with flooding tides occurs under the specified pressure boundary condition. No fluid flow was allowed across the sides or bottom of the simulation domain. This framework does not allow for the possibility of groundwater exchange between the marsh sediments and adjacent uplands, and is therefore most representative of a salt marsh island or a wide fringing marsh.

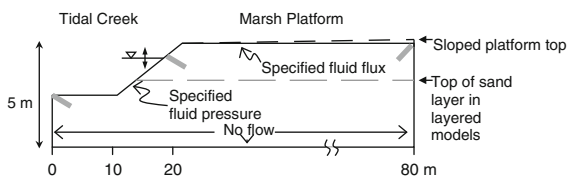

Fig. 1 Simulation domain and boundary conditions. *Gray tabs* indicate borders between types of boundary conditions. *Gray dashed line* indicates top of sand layer for layered models. *Black dashed line* indicates land surface for sloped platform models

At initial conditions, the hydraulic head throughout the domain was set equal to high tide for that simulation. Each simulation was run until a repeatable flow pattern developed for successive tidal cycles, i.e. until the transient simulation reached a quasi-steady condition. Initial conditions did not affect the final results.

We ran simulations using a range of marsh elevations, tidal amplitudes, and sediment permeabilities. The elevation of the marsh platform relative to MWL was varied from −0.75 to 1.75 m, and the tidal amplitude from 0.25 to 1.25 m. These ranges were designed to encompass temporal variations at a single site and spatial variations between different marshes. Combinations that would have allowed the creek bottom to be exposed at low tide were not simulated. Four sets of sediment properties were simulated: homogeneous marshes with isotropic permeabilities of (1) 10^{-11} m^2, (2) 10^{-12} m^2, and (3) 10^{-13} m^2, and (4) a marsh with a 2 m layer of low-permeability mud ($k = 10^{-14}$ m^2) overlying a sand layer with a permeability of 10^{-11} m^2. The permeabilities were based on common permeabilities for coastal sands (Wilson et al. 2008) and field observations (L. R. Gardner, unpublished data; Wilson, unpublished data). The porosity of the sand was 0.36, and the porosity of the mud was 0.65. The compressibilities of the sand and mud were 10^{-7} and 10^{-6} Pa^{-1}, respectively.

Once each simulation reached quasi-steady state, the total simulated discharge over a tidal cycle was calculated using a mass balance approach. The compressibility of water is much smaller than the compressibility of the sediments, so the total change in fluid volume over the time period can be approximated as the sum, over each element, of the change in saturation plus the change in elastic storage

$$V = \sum_{i=1}^{n} V_i \left(\phi \partial S_w - \frac{S_w}{\rho g} S_s \partial \sigma_e \right) \quad (6)$$

where V is the total volume, V_i is the volume of a finite element, ∂S_w is the change in water saturation and $\partial \sigma_e$ is the change in effective stress,

$$\partial\sigma_e = \partial\sigma_t - \partial P \quad (7)$$

where σ_t is total stress and P is pore pressure. The impact of neglecting changes in total stress can be easily assessed by setting $\partial\sigma_t = 0$ in Eq. 7. Note that the total discharge over a tidal cycle is not the same as the difference in water volume between high and low tide, because flow within the marsh interior lags the tidal signal, particularly in marshes where low-permeability muds overlie sands, as is common in the U.S. southeast. Our algorithm tracked inflow and outflow, and calculated the total flux accordingly.

As previously indicated, these simulations account for tidal fluctuations only, neglecting precipitation and evapotranspiration. In the models where the marsh platform was not inundated, tidally-driven fluctuations in the height of the water table decline with distance from the bank, leaving the water table at mean water level in the area of the domain farthest from the creek. In reality, a marsh platform that was never inundated by the tide would be subject to rainfall infiltration, which would cause the water table to rise and create a freshwater lens. The freshwater flow system would increase net discharge to the tidal creek, but it would not change the general effects of varying mean water level and tidal amplitude. Evapotranspiration could decrease the net discharge of groundwater in some instances, but in general losses to evapotranspiration are more likely to be made up by increasing recharge to the platform top during flooding than by decreasing discharge at the creek bank.

Nutrient data

Nutrient data summarized here have been collected in North Inlet estuary, South Carolina, USA, which is virtually free of anthropogenic point and nonpoint contamination from nutrients. North Inlet has a small undeveloped watershed of about 75 km^2. Consequently, mixing with surface fresh water input is minimal. The estuary contains about 18 km^2 of intertidal *S. alterniflora* marsh habitat (Morris et al. 2005) that experiences a regular semi-diurnal tidal pattern with a mean tidal range of approximately 1.4 m (Finley 1975). About 11.36×10^6 m^3 of water floods the estuary on an average tide (Nummedal and Humphries 1978), resulting in a residence time of 1 day for tidal creek water.

Pore-water samples have been collected monthly since December 1993 at four sites within North Inlet located in stands of *Spartina alterniflora* near creek-bank and interior marshes at Oyster Landing (33°21.024′N 79°25.427′W and 33°21.069′N 79°11.517′W, respectively) and Goat Island (1) (33°19.897′N 79°11.8759′W and 33°19.901′N 79°11.892′W). The collections were made using diffusion samplers that each held a vertical array of screened vials at sediment depths of 10, 25, 50, 75 and 100 cm. Pore-water samples were analyzed for ammonium and soluble reactive phosphorus according to methods in Strickland and Parsons (1968). Nutrient data and salinity were also analyzed from collections of creek water collected from a creek adjacent to Oyster Landing starting in 1982 as part of the Long Term Ecological Research (LTER) program at North Inlet (http://links.baruch.sc.edu/Data/index.html) and continuing through 2006 as part of NOAA's National Estuarine Research Reserve (NERR) program. Nutrient concentrations in surface and pore waters were summarized by taking the geometric means, which give better estimates of central tendency than arithmetic means when data are skewed (Sokal and Rohlf 1981). Nutrient concentrations in creek water at the Oyster Landing site in North Inlet were averaged by season of year for samples gathered from 1981 to 2006. Monthly nutrient concentrations (μmol/l) in pore water (1987–2007) were averaged over depth (10–100 cm), time (1987–2007), and site by season.

Results

Figure 2 shows flow patterns for an example simulation in which the marsh sediments consisted of a 2 m layer of mud ($k = 10^{-14}$ m^2) overlying sand ($k = 10^{-11}$ m^2) and in which the marsh platform sloped toward the creek. Groundwater flows downward through the mud, regardless of the stage of the tide, at rates nearing 0.01 m/day. The maximum flow rate in the sand layer was 3.8 m/day, at the water line on the creekbank at low tide. Flow rates in the sand layer at low tide exceeded 1 m/day in a zone that extended 15 m from the creekbank under the marsh platform. At other stages of the tide, flow rates in this zone were between 0.1 and 1 m/day. Unlike simulations with homogeneous sediments, flow remained focused within the permeable sand layer at depth

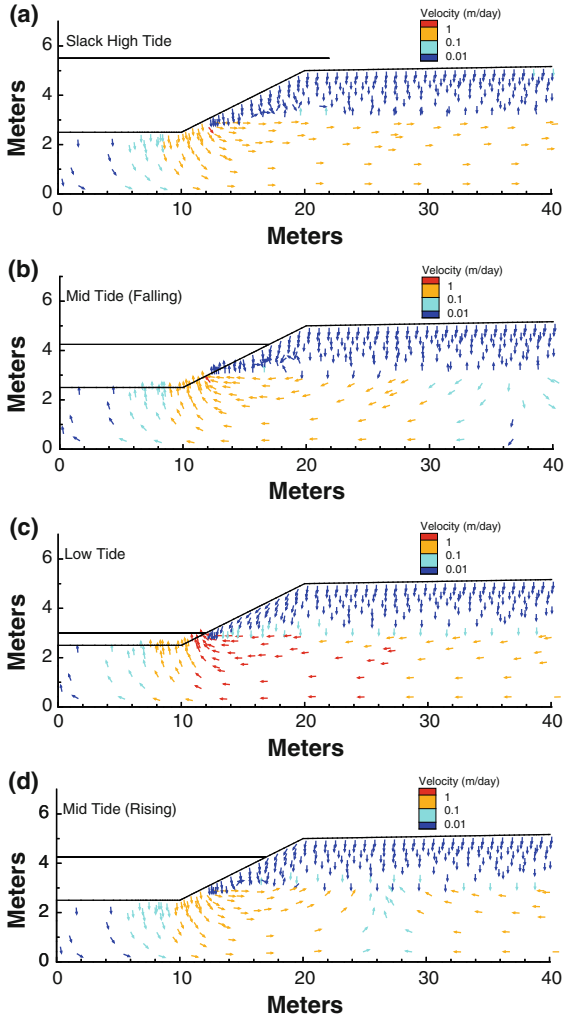

Fig. 2 Groundwater flow patterns from a layered platform with a sloping platform top. Tidal amplitude was 1.25 m, and the elevation of the platform (measured at the top of the creekbank) was 0.75 m. **a** High tide. **b** Mid-tide, falling. **c** Low tide. **d** Mid-tide, rising. Vertical exaggeration is twofold. Flow arrows are shown for only one of every four elements in the simulation

throughout the simulation rather than focusing at the water line in the creek bank.

We first present a series of simulations in which the tidal amplitude was set to 0.75 m and mean water level was varied. These simulations reveal discharges that range from less than 0.001 to 0.35 m^3 per m of creek bank per tidal cycle (Fig. 3). Simulations of the homogeneous higher-permeability marsh produced fluxes roughly four times as large as simulations in which permeability was reduced by an order of magnitude (Fig. 3a, b). Reducing the permeability by another order of magnitude reduced flow by another factor of four, indicating that flow is limited by permeability rather than the length of the tidal period for permeabilities less than 10^{-12} m^2. Fluxes from simulations with mud overlying permeable sand fell between the fluxes of the two more permeable models and showed somewhat different trends (Fig. 3d). The response of each system to a rise in MWL depended on the elevation of the marsh platform relative to mean high water (MHW) and on the stratigraphy of the system. For the homogeneous platforms, groundwater flushing increased if the rise in MWL caused a larger area of the creek bank or marsh platform to be inundated (Fig. 3a, b). The slope of the line (i.e., the increase in groundwater flushing per unit increase in MWL) depended on how much more of the platform was inundated at high tide. Accordingly, the greatest increase in groundwater flushing occurred in the flat-topped, homogeneous platforms when the relative elevation of the platform fell below 0.75 m, which suddenly allowed the full width of the platform to be completely inundated at high tide. At that threshold, a small (5 cm) decrease in the relative elevation of the marsh platform caused groundwater flushing to increase by 20, 22, and 24% for the permeable ($k = 10^{-11}$ m^2), less permeable ($k = 10^{-12}$ m^2), and least permeable ($k = 10^{-13}$ m^2) marshes, respectively. This effect was muted when a sloped top was added to the most permeable platform because the full width of the platform did not become fully inundated until the top of the creekbank rose only 0.25 m above MWL. This effect remained significant for the less permeable platforms because low permeability caused flow to be focused near the creekbank. Thus the exposure or inundation of areas far from the creekbank did not affect discharge significantly.

Once the marsh platform became regularly flooded at high tide, further increases in MWL caused overall flushing to decline steeply. The decline occurred because, as mean water level rose, low tide exposed increasingly small areas of the creek bank for increasingly short periods of time. For the simulations with more permeable sediments or with layered stratigraphy, slightly more flow occurred in the sloped platforms than in the flat-topped platforms because the slope caused a small lateral hydraulic gradient to develop across the marsh. This effect disappeared for the simulations with the lowest permeabilities (10^{-13} m^2), because most flow was

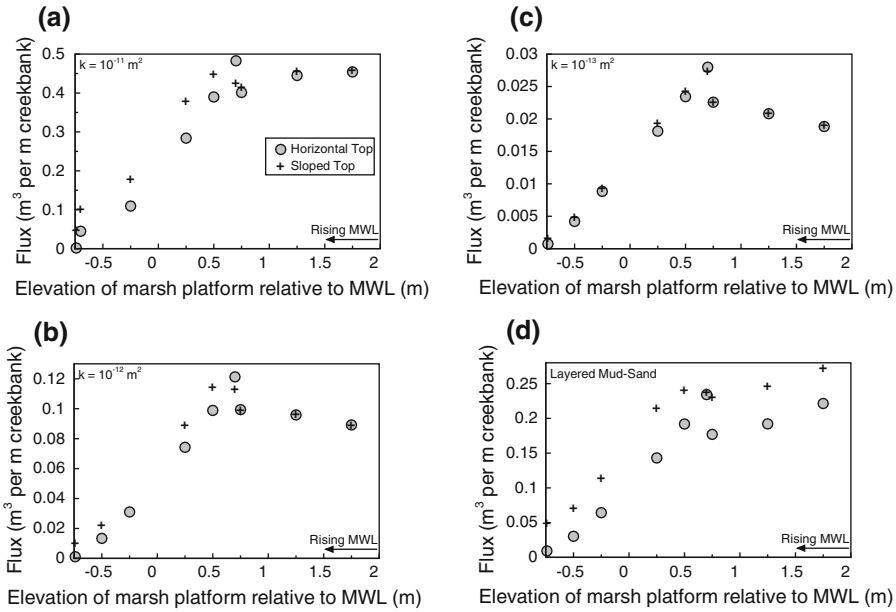

Fig. 3 Total groundwater discharge per tidal cycle as a function of the platform elevation relative to MWL. The tidal amplitude was 0.75 m, and each symbol represents a simulation with a different platform elevation. **a** High permeability ($k = 10^{-11}$ m^2) homogeneous sediments. **b** Intermediate-permeability ($k = 10^{-12}$ m^2) homogeneous sediments. **c** Low-permeability ($k = 10^{-13}$ m^2) homogeneous sediments. **d** Layered sediments ($k_{mud} = 10^{-14}$ m^2, $k_{sand} = 10^{-11}$ m^2). For the sloped platforms, the relative elevation of the marsh platform was measured from the top of the creek bank to MWL. Thus the flat marsh platforms were completely inundated at high tide when the relative elevation was less than 0.75 m. The sloped platforms were partially inundated for relative elevations of 0.25–0.75 m and became completely inundated when the relative elevation was less than 0.25 m

confined to the creekbank, which was unaffected by the slope of the marsh platform. The minimal groundwater flux calculated when the relative platform elevation was −0.75 m (below MWL) reflects flow due only to the compressibility of water in response to changes in the weight of overlying water during tidal fluctuations.

The slight differences in the shapes of the curves in Fig. 3a, b stem from the fact that tidal fluctuations propagate quickly into the more permeable platform, so that significant flow occurred beyond the sloping creekbank. In the less permeable platform, most flow occurred within a few meters of the creek bank, so the shape of the creekbank played a more important role.

In the layered platforms, decreases in the relative elevation of the marsh platform caused groundwater flushing to decrease except when the top of the platform started to become inundated at high tide (relative elevation less than 0.75 m). In the layered models, most flow focused in the permeable sand layer, which outcropped in the lowest 0.5 m of the creek bank. Thus at the lowest water levels the large hydraulic gradients that develop surrounding the water line were in the permeable sand layer. As the MWL increased relative to the elevation of the platform top, the largest hydraulic gradients migrated up into the less permeable mud, and the connection to the sand layer was diminished.

We also tested the effects of increasing the tidal amplitude while the elevation of the platform relative to MWL was held constant. In these simulations, increases in tidal amplitude caused the total discharge to increase regardless of the composition or shape of the marsh platform (Fig. 4). The increase was linear for simulations in which high tide did not inundate the marsh platform. Groundwater exchange increased as the top of the platform started to become inundated at high tide, and the increase was again greatest for the flat-topped models. Thereafter a linear trend was re-established, but the slope of the line decreased after the platform was inundated. Before the platform was inundated, every increase in tidal amplitude affected new areas of the creek bank at both high and low tides, but once the platform was inundated at

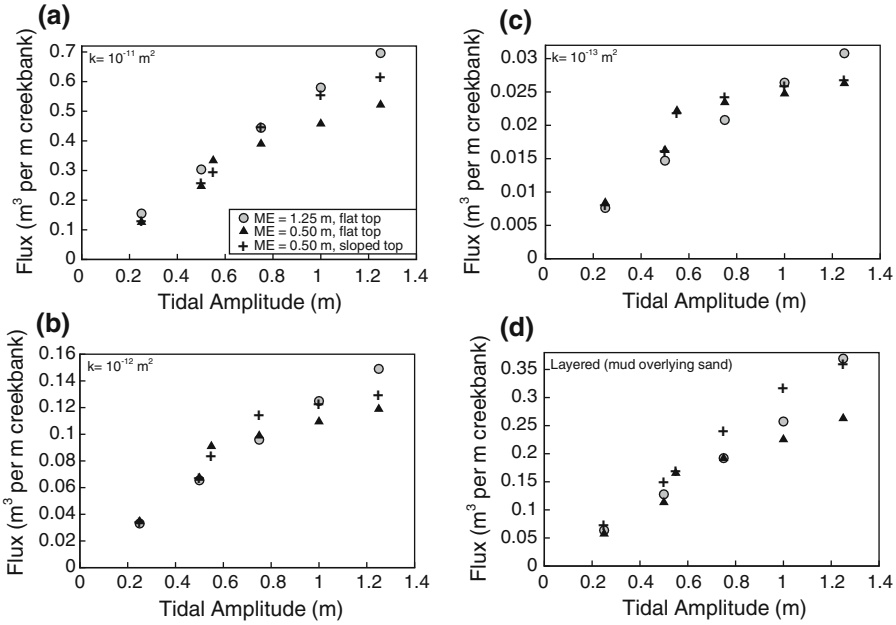

Fig. 4 Total groundwater discharge per tidal cycle as a function of tidal amplitude. **a** Permeable homogeneous sediments. **b** Intermediate-permeability homogeneous sediments. **c** Low-permeability homogeneous sediments. **d** Layered sediments. For simulations with a relative platform elevation of 1.25 m, the marsh platform was never inundated. For those with a platform elevation of 0.50 m, flat marsh platforms were inundated when the tidal amplitude exceeded 0.50 m; sloped marsh platforms were fully inundated when the amplitude exceeded 1.0 m

high tide increases in tidal amplitude only flushed new areas of the creek bank at low tide. In the lower permeability and layered models, the trend was slightly non-linear for simulations in which the platform was inundated at high tide, again reflecting the sensitivity of these models to the geometry and composition of the creekbank.

Concentrations of ammonium and soluble reactive phosphorus at North Inlet are greater in marsh pore water than in creek water (Fig. 5). In marsh sediments, the average concentration of ammonium in the pore water, 25 µmol/l, was 15.6 times greater than concentrations observed in the tidal creek at Oyster Landing, which is the most landward sampling station and the creek environment with the highest nutrient concentrations (Morris 2000). The mean nitrate-nitrite concentration in creek water was low, 0.4 µmol/l, and in pore water was typically below detection (data not shown). Soluble reactive phosphorous averaged 3.7 µmol/l in marsh pore water and 0.3 µmol/l in surface water from the creek (Fig. 5). N:P ratios, 6.8 in marsh pore water and 5.3 in the creek, were low, which is consistent with nitrogen limitation of primary producers in this system (Lewitus et al. 1998; Morris 1988).

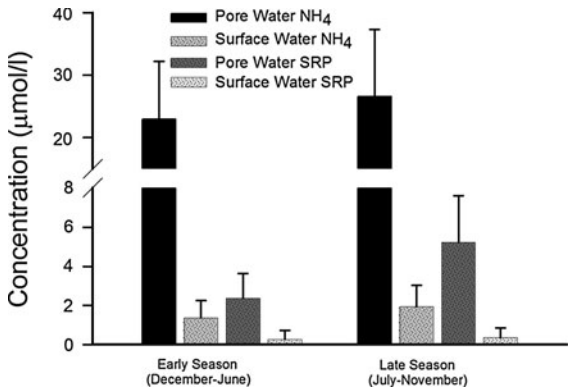

Fig. 5 Average seasonal nutrient concentrations in salt marsh pore water and surface water from North Inlet, SC

Discussion

Our modeling results suggest a simple explanation for the differences in the effect of increasing MWL between field observations (Morris and Haskin 1990; Morris 2000) and prior simulation results (Harvey et al. 1987). The Goat Island monitoring site at North Inlet is located in the marsh surrounding Goat Island, a sandy paleo-beach ridge. In this location the marsh slopes upward toward the island, and the upland border of the marsh is characterized by salt crusts and a community of *Salicornia virginica*. This site is not inundated by every high tide, so, according to our results, increases in MWL should cause larger areas of the marsh to be inundated at high tide, which increases porewater flushing. In contrast, Harvey

et al. (1987) reported that the marsh they simulated was dominated by low marsh that was inundated roughly 340 days per year. Furthermore the marsh was bordered by a narrow high marsh and hillslope, suggesting that increases in MWL could not have inundated significantly larger areas even if the marsh had been equilibrated higher in the tidal frame.

The individual simulations presented here allowed us to calculate groundwater fluxes that would occur for a very simple sinusoidal tidal signal that remained stable over long periods. In real tidal wetlands groundwater fluxes depend on the history of the system, which may include tidal signals that vary over time scales of days (storm surge), weeks (spring-neap cycles), months (seasonal changes), and years (e.g. lunar nodal cycles). This raises the question of how long it takes for a real marsh to equilibrate to new tidal signals, and this time can be estimated based on how long it took for each simulation to equilibrate. For models in which the marsh platform was never inundated, the highest-permeability models reached equilibrium in less than 5 days. For each order of magnitude decrease in permeability, the equilibration time increased by roughly a factor of 10, although the portion of the model nearest the creek (i.e. where tidal fluctuations affected flow) reached equilibrium much more rapidly. When the marsh platform was inundated, the simulations reached equilibrium quickly, within only a few tidal cycles, regardless of the permeability. Thus, in real marshes, the 'memory' or hysteresis of the system probably depends on its elevation relative to mean high water. In low marshes, which are commonly inundated at high tide, this period is likely very short, on the order of days at most. In high marshes this period is likely limited to the time since the last series of inundating spring tides, a few weeks at most. These simulations do not quantitatively estimate the groundwater fluxes that would be generated in a real system by, for example, storm surge. They do, however, provide a clear basis for interpreting the impact of variations in real tidal signals within and between different marsh systems. We first consider the implications of these results for nutrient fluxes at North Inlet, then describe the broader implications for other marsh systems.

These results suggest that groundwater export from tidal marshes can be a significant source of nutrients in non-river-dominated estuaries such as North Inlet. We can estimate this flux by applying the range of discharges typical of North Inlet conditions to the concentrations of ammonium and phosphate in marsh pore water (Fig. 5). Given a mean platform elevation of 30 cm (Morris et al. 2005) and tidal amplitude of 70 cm (Morris 2000) at North Inlet, groundwater discharge was estimated at $\sim$0.015 to 0.3 m^3 per meter of creek bank per tidal cycle (Fig. 3). We computed total creekbank length using a marsh island creek density of 0.013 m/m^2 (Novakowski 2004), marsh area of 17.9 km^2 and inter-island creek length of 29 km (Morris et al. 2005). The resulting fluxes of 0.44 to 8.4 L/m^2 per tide bracket the prior estimate of Morris (1995; 5 L/m^2 per tide) and are somewhat lower than those of Krest et al. (2000; 10 to 20 L/m^2 per tide). This gave estimates of gross ammonium export in pore water discharge of between 200 and 3900 mol/tide, and soluble reactive phosphorus export of 29–580 mol/tide. Morris (2000) estimated a net export from North Inlet estuary of 2900 and 860 mol/tide of ammonium and phosphorus, respectively, based on a mass balance of these constituents in the ebbing and flooding tides.

Our model estimates and the mass balance calculations of ammonium and phosphorus export are consistent to an order of magnitude. An unknown fraction of the inorganic nutrients exported from the marsh is assimilated by phytoplankton within the estuary and is either redeposited onto the marsh, exported as particulate matter, or excreted by bivalves (Dame et al. 1985). Thus, nutrient export from the estuary to the coastal ocean should be less than nutrient discharge from the marshes. If all calculations are correct, then there appears to be an export of phosphate from the estuary that cannot be accounted for by tidally-driven creek discharge. Nevertheless, export by drainage of inorganic forms of nitrogen and phosphorous from the marshes is quite large relative to net export from the estuary. The dominance of ammonium in the estuary provides additional evidence for the importance of nutrient export from these marshes (Fig. 5), because streams and rivers are typically dominated by nitrate-nitrogen, not ammonium (Peterson et al. 2001; Meybeck 1982; Mayer et al. 2002). Finally, it should be noted that the pore water concentrations of ammonium that we used in our calculations are actually lower than those reported by Whiting and Childers (1989) for a creekbank in North Inlet, while their reported phosphate concentrations were consistent with ours.

We also note that nutrient export from marshes is probably not a major contributor to the nutrient budgets of river-dominated estuaries. In the context of total reactive nitrogen export to the coastal zone from the conterminous United States of 5 Tg N/year (Howarth et al. (2002), its 20 $\times$ 10^3 km^2 area of tidal wetlands (Bridgham et al. 2006), total ammonium export from tidal wetlands should range from 0.02 to 0.76% of riverine export, depending on the drainage rate (0.015–0.3 m^3 m^{-1} $year^{-1}$).

We can make an important generalization about the behavior of nutrients in this system. Firstly, with the exception of nitrate, this marsh cannot assimilate a net quantity of dissolved inorganic nitrogen or phosphorous from the water column. The concentration gradients are in the wrong direction for transport of ammonium and dissolved phosphate into the marsh sediment, and there is clearly a net advection of nutrients from the marsh to the tidal creeks, which the model calculations demonstrate. However, in situations where flood waters are dominated by nitrate-nitrogen, a great deal of this nitrate is probably denitrified in marsh sediments. Moreover, marshes can trap and bury considerable quantities of particulate matter. Nevertheless, there is very likely a substantial nutrient subsidy to estuarine waters from surrounding marshes, and the net balance between dissimilatory nitrate reduction by marshes, particle trapping, and ammonium discharge remains an open question. This represents a significant revision of the notion that wetlands are the kidneys of the landscape (Mitsch and Gosselink 2000), but the revision may apply only to salt water wetlands because of the unique chemistry of their soils.

Given the importance of groundwater export of nutrients described above, this work also suggests that seasonal variations in MWL, which typically rise 30 cm in the summer due to steric effects, could contribute significantly to seasonal variations in nutrient exchange for marshes. Ground water discharge could increase during the summer for marshes that are equilibrated near mean high water, if that increase in MWL caused greater portions of the marsh to be inundated or if the marsh were inundated more frequently. For marshes like North Inlet, however, where the average relative elevation is closer to average MWL (0.30 m; Morris et al. 2005), the seasonal rise in MWL could cause a substantial decrease in nutrient export.

Variations in tidal amplitude should also significantly influence nutrient exchange in intertidal wetlands. For marshes that are otherwise similar in hydrology and stratigraphy, it is not surprising that groundwater and nutrient exchange should be much larger in macrotidal systems than in microtidal systems. Less apparent, yet potentially equally important, is that greater groundwater flushing should occur in marshes during spring tides than neap tides, regardless of the elevation or composition of the marsh platform. This effect will be maximized in marshes with platform elevations near mean high water, i.e. those that are inundated by spring tides but not neap tides. The impact of this increased flow on nutrient concentrations in surface water is difficult to predict, however, because increases in tidal amplitude also increase the volume of the tidal prism. In the Parker River estuary, Massachusetts, marshes are typically flooded during spring tides but not during neap tides, and observed surface water nutrient concentrations are lower during spring tides than neap tides (Vörösmarty and Loder 1994). Groundwater exchange will also likely vary spatially within estuaries owing to variations in tidal amplitude between the mouth and landward portions of the estuary.

Finally, relative sea-level rise could have a significant impact on estuarine water quality. For the majority of marshes that currently lie between mean sea level and mean high water level (McKee and Patrick 1988), relative sea-level rise should substantially increase flooding of the marsh platform at high tide and cause groundwater and nutrient discharge from the marsh to increase. Further increases in mean sea level relative to the marsh surface cause groundwater flushing to decrease. Consequently, sea-level rise could impact estuaries in two stages. In stage one, rising sea level should increase the discharge of ground water from coastal wetlands, possibly leading to a substantial fertilization of estuaries and rising pelagic productivity. In the final stage, as rising sea level overtakes marshes unable to keep pace, ground water and nutrient discharge from marshes and pelagic productivity would decline. This effect may vary spatially within an estuary as well; at North Inlet the central marsh islands are low enough in the tidal frame that increases in MWL will decrease groundwater exchange, but higher fringing marshes should experience increases in groundwater exchange.

Conclusions

Groundwater flow is an important control on nutrient exchange between salt marshes and adjacent estuaries, and this exchange is influenced by long- and short-term variations in the tidal signal. Calculations based on conditions typical of North Inlet estuary, SC, confirm that discharging porewaters introduce significant nutrients to estuarine systems. Fluxes of nutrients from marshes are less important in river-dominated systems. Increases in tidal amplitude increase the volume of groundwater exchange, with a sharp increase in flushing when the marsh platform becomes inundated at high tide. Increases in mean water level cause relatively small changes in groundwater flushing when the marsh platform is never inundated, but flushing can increase significantly when the platform becomes inundated at high tide, depending on the slope and stratigraphy of the marsh platform. After the platform becomes fully inundated at high tide, further increases in mean water level cause groundwater flushing to decline.

These results also suggest that the effects of rising sea level on marsh nutrient and salt dynamics will depend on the relative elevation of those marshes. Seasonal and climate-related rises in mean water level could increase groundwater and nutrient fluxes if that rise causes the marsh platform to be inundated more frequently or if it causes greater areas of the marsh to be inundated at high tide. Low marsh islands that are already inundated during most high tides, however, would experience decreased groundwater flushing. Corresponding decreases in nutrient export could affect nutrient budgets, and thus fertility, in adjacent surface waters.

Acknowledgments We thank two anonymous reviewers for very helpful reviews. This material is based upon work supported by the National Science Foundation under Grants No. EAR-0711301 (AMW), DEB-0316429 (JTM) and OCE-0423565 (JTM) and by South Carolina Sea Grant Project R/ER-30 to AMW and JTM. This is contribution 1621 of the Belle W. Baruch Institute for Marine and Coastal Sciences.

References

Bridgham SD, Megonigal JP, Kelley JK, Bliss NB, Trettin C (2006) The carbon balance of North American wetlands. Wetlands 26:889–916

Dame RF, Wolaver TG, Libes SM (1985) The summer uptake and release of nitrogen by an intertidal oyster reef. Neth J Sea Res 19:265–268

Fang CS, Wang SN, Harrison W (1972) Groundwater flow in a sandy tidal beach 2. Two-dimensional finite element analysis. Water Resour Res 8(1):121–128

Finley R (1975) Hydrodynamics and tidal deltas of North Inlet, South Carolina. In: Cronin E (ed) Estuarine research. Academic Press, New York, pp 277–291

Gardner WR (1958) Some steady state solutions of unsaturated moisture flow equations to applications to evaporation from a water table. Soil Sci 82:228–232

Gardner LR (2005) Role of geomorphic and hydraulic parameters in governing pore water seepage from salt marsh sediments. Water Resour Res 41:W07010. doi: 10.1029/2004WR003671

Gardner LR (2007) Role of stratigraphy in governing pore water seepage from salt marsh sediments. Water Resour Res 43:W07502. doi:10.1029/2006WR005338

Gardner LR, Reeves H (2002) Spatial patterns in soil water fluxes along a forest-marsh transect in the southeastern United States. Aquat Sci 64:141–155

Gardner LR, Wilson AM (2006) Comparison of four numerical models for simulating seepage from salt marsh sediments. Estuar Coast Shelf Sci 69:427–437

Harvey JW, Germann PF, Odum WE (1987) Geomorphological control of subsurface hydrology in the creekbank zone of tidal marshes. Estuar Coast Shelf Sci 25:677–691

Hemond HF, Fifield JL (1982) Subsurface flow in a salt marsh peat: a model and field study. Limnol Oceanogr 27(1): 126–136

Howarth RW, Boyer EW, Pabich WJ, Galloway JN (2002) Nitrogen use in the United States from 1961–2000 and potential future trends. Ambio 31:88–96

Howes BL, Howarth RW, Teal JM, Valiela I (1981) Oxidation-reduction potentials in a salt marsh: spatial patterns and interactions with primary production. Limnol Oceanogr 26(2):350–360

King GM, Klug M, Weigert RG, Chalmers AG (1982) Relation of soil water movement and sulfide concentration to *Spartina alterniflora* production in a Geogia salt marsh. Science 218:61–63

Krest J, Moore WS, Gardner LR, Morris JT (2000) Marsh nutrient export supplied by groundwater discharge; evidence from radium measurements. Global Biogeochem Cycles 14(1):167–176

Lewitus AJ, Koepfler ET, Morris JT (1998) Seasonal variation in the regulation of phytoplankton by nitrogen and grazing in a salt-marsh estuary. Limnol Oceanogr 43:636–646

Li H, Li L, Lockington D (2005) Aeration for plant root respiration in a tidal marsh. Water Resour Res 41:W06023. doi:10.1029/2004WR003759

Mayer B et al (2002) Sources of nitrate in rivers draining sixteen watersheds in the northeastern U.S.: isotopic constraints. Biogeochemistry 57/58:171–192

McKee KL, Patrick W (1988) The relationship of smooth cordgrass (*Spartina alterniflora*) to tidal datums: a review. Estuaries 11:143–151

Medelssohn IA, Morris JT (2000) Ecophysiological controls on the growth of *Spartina alterniflora*. In: Weinstein NP, Kreeger DA (eds) Concepts and controversies in tidal

marsh ecology. Kluwer Academic Publishers, Dordrecht, pp 59–80
Medelssohn IA, McKee KL, W H Patrick J (1981) Oxygen deficiency in *Spartina alterniflora* roots: metabolic adaptation to anoxia. Science 214:439–441
Meybeck M (1982) Carbon, nitrogen, and phosphorus transport by world rivers. Am J Sci 282:401–450
Mitsch WJ, Gosselink JG (2000) Wetlands. Wiley, Hoboken
Morris JT (1988) Pathways and controls of the carbon cycle in salt marshes. In: Hook DD et al (eds) The ecology and management of wetlands, vol 1: Ecology of wetlands. Croom Helm, London
Morris JT (1995) The mass balance of salt and water in intertidal sediments: results from North Inlet, South Carolina. Estuaries 18(4):556–567
Morris JT (2000) Effects of sea-level anomalies on estuarine processes. In: Hobbie J (ed) Estuarine science: a synthetic approach to research and practice. Island Press, Washington, pp 107–127
Morris JT, Haskin B (1990) A 5-yr record of aerial primary production and stand characteristics of *Spartina alterniflora*. Ecology 71(6):2209–2217
Morris JT et al (2005) Integrating LiDAR elevation data, multispectral imagery and neural network modelling for marsh characterization. Int J Remote Sens 26:5221–5234
Novakowski KI, Torres R, Gardner LR, Voulgaris G (2004) Geomorphic analysis of tidal creek networks. Water Resour Res 40:W05401. doi:10.1029/2003WR002722
Nunmedal D, Humphries SM (1978) Hydraulics and dynamics of North Inlet, South Carolina, 1975-1976. GITI report 16. Department of the Army Corps of Engineers, Coastal Engineering Research Center, Fort Belvoir, VA and U.S. Army Engineer Waterways Experiment Station, Vicksburg, MS
Nuttle WK (1988) The extent of lateral water movement in the sediments of a New England salt marsh. Water Resour Res 24(12):2077–2085
Peterson BJ et al (2001) Control of nitrogen export from watersheds by headwater streams. Science 292:86–90
Reeves H, Thibodeau PM, Underwood RG, Gardner LR (2000) Incorporation of total stress changes into the ground water model SUTRA. Ground Water 38(1):89–98
Sokal RR, Rohlf FJ (1981) Biometry: the principles and practice of statistics in biological research. W.H. Freeman and Company, San Francisco, p 859
Strickland TD, Parsons TR (1968) A practical handbook of seawater analysis. Bull Fish Res Board Can 167:1–311
Stumpf RP, Haines JW (1998) Variations in tidal level in the Gulf of Mexico and implications for tidal wetlands. Estuar Coast Shelf Sci 48:165–173
Valiela I, Teal J, Deuser W (1978) The nature of growth forms in the salt marsh grass *Spartina alterniflora*. Am Nat 112: 461–470
Vörösmarty C, Loder TI (1994) Spring-neap tidal contrasts and nutrient dynamics in a marsh-dominated estuary. Estuaries 17(3):537–551
Voss CI, Provost AM (2002) A model for saturated-unsaturated, variable-density ground-water flow with solute or energy transport. U.S. Geological Survey water-resources investigations report 02-4231
Whiting GJ, Childers DL (1989) Subtidal advective water flux as a potentially important nutrient input to southeastern U.S.A. saltmarsh estuaries. Estuar Coast Shelf Sci 28: 417–431
Wilson AM, Gardner LR (2006) Tidally driven groundwater flow and solute exchange in a marsh: Numerical simulations. Water Resour Res 42:W01405. doi:10.1029/2005WR004302
Wilson AM, Huettel M, Klein S (2008) Grain size and depositional environment as predictors of permeability in coastal marine sands. Estuar Coast Shelf Sci 80(1): 193–199